



Water remediation by UV–vis/H₂O₂ process, photo-Fenton-like oxidation, and zeolite ZSM5

Fabiola Mendez-Arriaga*, Rafael Almanza

Instituto de Ingeniería, Coordinación de Mecánica y Energía, Universidad Nacional Autónoma de México UNAM, Circuito exterior s/n, Cd. Universitaria, Coyoacán 04510 México, D.F, México

Email: fmendoza@iingen.unam.mx

Received 14 February 2012; Accepted 6 June 2013

ABSTRACT

The present work shows the application of the UV–vis/H₂O₂ process, Fenton and photo-Fenton-like reactions in presence of zeolite material ZSM5 in the degradation of a pharmaceutical pollutant recently found in environmental aquatic systems, the anti-inflammatory drug naproxen (NPX). Three commercial iron oxide powders (hydrated hematite, hematite, and magnetite) for Fenton-like reaction were tested against 10 mg L⁻¹ of NPX. An UV–vis simulator source was employed in order to contrast the performance of the photo-Fenton-like reaction during 120 min of irradiated conditions in a no-buffered almost neutral pH 6.5 ± 0.5. ZSM5 zeolite was tested as adsorbed material in mechanical mixtures with or without iron oxide powders in order to improve the physical removal along with the oxidative stress. Effects of non-photocatalytic control test (such as UV–vis photolysis, H₂O₂ oxidation, and oxide iron complex formation) were previously evaluated. Negligible effect was evidenced for Fenton-like reaction and adsorption in dark conditions by the use of neither iron oxide species nor zeolite (<0.01 mmol NPX L⁻¹ min⁻¹). In contrast, the photo-Fenton-like reaction promotes the total elimination of initial 10 mg L⁻¹ of NPX with a concomitant 50–60% of mineralization by the use of Fe₂O₃ and Fe₃O₄, respectively, with 18 and 14 mmol L⁻¹ min⁻¹ initial NPX degradation rate. Improvement of dissolved organic carbon (DOC) reduction by adsorption due to the presence of ZSM5 was not observed under illuminated conditions and biodegradable character of the final effluent was not improved. The presence of a heterogeneous material such as zeolite ZSM5, promotes only a benefit effect on DOC removal in absence of H₂O₂ reagent and results are antagonist to Fenton-like and photo-Fenton-like reactions due to the well-differentiated reaction mechanism and the concomitant likely dissimilar by-products generated. Residual by-products are not suitable for a post-biological operation due to the formation of recalcitrant polymers not further degraded by photo-Fenton-like reaction with iron oxides.

Keywords: Photo-Fenton like reaction; Iron oxides; Organic pharmaceutical pollutants

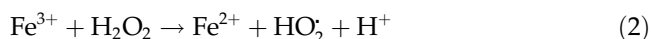
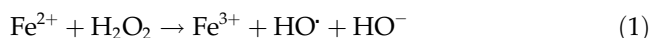
1. Introduction

The pharmaceutical industry started a significant development and production at the end of the

nineteenth century; however the subsequent environmental problem related to the presence of residual pharmaceuticals compounds as pollutants has been recognized very recently [1]. Compounds such naproxen (NPX), a non-steroidal anti-inflammatory

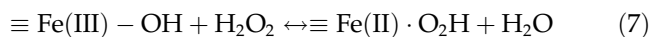
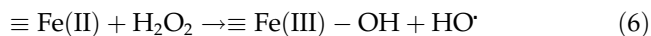
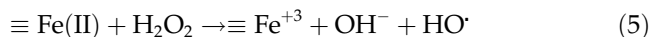
*Corresponding author.

drug, among others, have been found in solid and aqueous phases in the environment, principally as a result of an incomplete degradation process in wastewater municipal plants [2]. On the other hand, advanced oxidation processes (AOPs) have acted as alternative technologies for depletion of pharmaceutical recalcitrant pollutants. APOs are applied to the treatment of organic contaminants in water, soils, and air, based on the presence and reactivity of hydroxyl radicals (HO^\cdot) generated under atmospheric or super/subcritical conditions of temperature and pressure with or without catalyst and/or reactive energy (electrochemical, UV-vis or ultrasounds) [3]. Reaction between iron salts and hydrogen peroxide in acidic media, the named Fenton reaction, is one of the most applied and promising AOP. Fenton and photo-Fenton reactions have been applied for removal of emerging pharmaceutical contaminants [4,5]. Fenton classical reaction is based on the catalytic cycle between Fe^{+2} and Fe^{+3} in acid media with the concomitant H_2O_2 depletion to form the highly oxidant radical HO^\cdot [3].

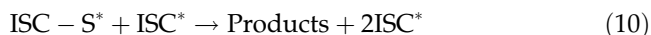


The use of both reagents (ionic iron and H_2O_2), as industrial treatment, has several inherent unsolved problems and considerable technical restrictions. For example, Fenton reaction can be early inactivated as consequence of organic iron-complex formation stopping the hydrogen peroxide consumption. On the other hand, formation of considerable iron-sludge amounts and strict control of pH (acid media) do not make yet tangible the industrial application of Fenton reaction for wastewater. An approximation of Fenton reaction has been conducted by the use of iron oxides, the named Fenton-like process. Iron oxides are natural, abundant, and inexpensive. They are produced from the hydrolysis of aqueous Fe^{3+} solutions before precipitation and are practically insoluble in water. The most common iron oxide minerals are wustite (FeO), goethite (FeO-OH), hematite (Fe_2O_3), and magnetite (Fe_3O_4). In contrast with the well-interpreted initial Fenton reaction process, the mechanism of HO^\cdot generation on iron oxide surfaces is not well understood [6]. The hydrogen peroxide depletion by oxide iron catalytic surfaces has been described by several authors, yet well-differentiated mechanisms have been proposed depending on the particular iron oxide species. Some authors suggest an initiated radical reaction involving $\equiv\text{Fe(III)}$ species which goes further

oxidation of the organic pollutant analogous to Fenton thermal reaction [7]:



The process apparently involves HOO^\cdot hydroperoxyl and HO^\cdot hydroxyl radicals. In contrast, Andreozzi et al. [8] report a non-radical mediated reaction but also an initiated process by the formation of an inner-sphere complex (ISC) between $\equiv\text{Fe(III)-OH}$ groups and H_2O_2 on the oxide surface:



where (*) indicates free catalyst active sites and (S) indicates substrate. The surface complex may be regarded as a ground-state, mediating a reversible electronic ligand-to-metal charge transfer (LMCT).

Iron oxides, as active catalysts in the Fenton-like reaction, have showed controversial results in water treatment applications. Garrido et al. [9] suggest that iron oxides fill complete requirements in pollutant removal, stability, high H_2O_2 conversion, minimum decomposition, and reasonable cost. The oxidation by catalyzed process by iron-oxide minerals (especially by use of goethite) has been reported in degradation of several organic compounds [8,10–15], etc. On the other hand, in contrast, several authors report the ineffective H_2O_2 consumption with its concomitant poor HO^\cdot generation by the presence of iron oxides as magnetite [16–18]. Few applications of Fenton-like reaction to pharmaceutical pollutants have been reported. However an interesting application, described by Melero et al. [19], involves the catalytic wet peroxide oxidation in the presence of $\text{Fe}_2\text{O}_3/\text{SBA15}$ nanocomposite against industrial pharmaceutical wastewaters.

On the other hand, the photo-Fenton-like reaction by the use of UV-vis radiation, accelerates the

reduction of Fe^{+3} to Fe^{+2} , analogous to the described by Pignatello et al. [20]. In photo-Fenton reaction, the aqueous Fe^{+3} solutions (as ferric oxyhydroxides), $\text{Fe}(\text{OH})^{2+}$ is the dominant species and it photolyzes to produce hydroxyl radicals. Moreover, Fe^{+3} complexes undergo LMCT excitation, dissociating to give Fe^{+2} and an oxidized ligand. The photochemical properties of iron oxides are also associated to the analogous activity of photoproducing e^-/h^+ couple observed in the photocatalytic semiconductors such as TiO_2 . For instance, Fe_2O_3 (band gap around 2.2 eV) has shown potential semiconductor character for interfacial electron transfer in compounds such as bisulfate, mono or poly-carboxylate compounds, or fluoroacetic acids [7,30]. Also, special photochemical properties of Fe(III)–OH complexes, Fe(III) oxides, or Fe(III) hydroxides have been widely shown [29,31], particularly for oxides such $\alpha\text{-Fe}_2\text{O}_3$, $\gamma\text{-Fe}_2\text{O}_3$, $\alpha\text{-FeOOH}$, $\beta\text{-FeOOH}$, and $\gamma\text{-FeOOH}$. The photoreduction of Fe^{+3} to Fe^{+2} is achieved by its electron acceptor propriety by photo-induced LMCT from absorbed organic reductant to a Fe(III) center on the metal oxide surface. There exist few reported evidences on the photo-Fenton-like applications against pharmaceutical pollutant by the use of iron oxide minerals; however relevant information for depletion of Procaine Penicilline G formulation has been reported by Arslan-Alaton and Gurses [21].

On the other hand, several natural or synthetic solids in pillared interlayered or porous forms containing iron species (e.g. zeolites) have been tested for the oxidation of organic compounds by catalyzed decomposition of H_2O_2 by ionic, hydroxide, or oxide forms in heterogeneous phase [18]. In particular, a wide variety of zeolites has been used for this propose [22,23]. Furthermore, most of these solid materials have shown significant adsorbing properties resulting in an increase of the effective organic concentration near the catalytic site [24].

Therefore, in this work was proposed to study the degradation of a persistent relevant pharmaceutical pollutant NPX by Fenton-like and photo-Fenton-like reaction by use of three commercial iron oxides (hyd Fe_2O_3 , Fe_2O_3 , and Fe_3O_4) as well as by mechanical mixtures between such oxides and zeolite ZSM5 in order to evaluate the synergic or antagonist effect, in presence of H_2O_2 and UV–vis solar simulated irradiation.

2. Experimental

2.1. Materials and analytical methods

NPX (Sigma) was used as received. Table 1 shows the most relevant physicochemical properties of NPX.

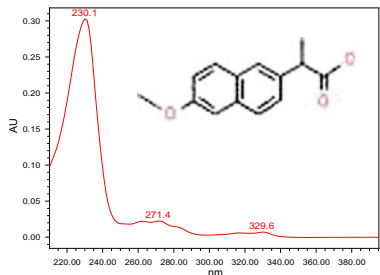
The oxide iron species hydrated hematite (hyd- Fe_2O_3), hematite (Fe_2O_3), and magnetite (Fe_3O_4) were supplied by Suministro de Especialidades SA de CV and used without further treatment. H_2O_2 (30% purity) was J. T. Backer and zeolite Na-ZSM5 (Zeocat PZ-2/25)—hereafter referred as Z—was obtained from Zeochem and used as received. Table 2 shows the physicochemical characteristics of iron oxides and Z employed. Deionized water quality was used in all experiments and carried out at least twice.

NPX concentration was monitored after sample-filtration (HAWP Millipore 0.45 μm) in a high performance liquid chromatographic instrument (HPLC) Agilent using a C_{18} ACE column. An isocratic flow rate of 1 mL min^{-1} was used and the composition of the mobile phase was maintained with methanol 60%, acetonitrile 15%, and formic acid (0.1%) 25%. The temperature of the analysis was controlled to 25°C and the injection volume was fixed to 10 μL . The detection wavelength was adjusted to 230 nm into a retention time of approximately 3 min. The detection limit was 0.5 mg L^{-1} with an accuracy of 0.2 mg L^{-1} . Dissolved organic carbon (DOC) measurements were obtained by a TOC-Shimadzu instrument model TOC-V_{CNS}. Both, HPLC and DOC determinations were immediately analyzed after filtration and H_2O_2 deactivation with sodium tiosulphate solutions (J.T. Backer) 0.1 N. H_2O_2 residual concentration was measured by $\text{Mo}_7\text{NH}_4\text{O}_{24}$ (J.T. Backer) 0.01 M and KI (J.T. Backer) 0.1 M by photometric method recorded after 2 min at 365 nm in a Hach 5120 spectrophotometer [25]. BOD₅ determinations were carried out according to the standard methods (5210-B) by a respirometric process and Oxitop® equipment with a Poliseed® reference inoculums, $\text{FeCl}_3 \cdot 6\text{H}_2\text{O}$ (J.T. Backer), $\text{MgSO}_4 \cdot 7\text{H}_2\text{O}$ (J.T. Backer), CaCl_2 (J.T. Backer) as nutrients, phosphate buffer (WTW), and denitrification solution (WTW) used previously complete the H_2O_2 inactivation. The Oxitop system is based on pressure measurement via piezoresistive electronic sensors. A measuring range of 0–40 mg L^{-1} was selected.

2.2. Experimental procedures





Defined initial NPX concentration was spiked in deionized water (total volume 1 L) during 120 min since total dissolution (unbuffered natural pH 6.5 \pm 0.5). In dark conditions, mechanical mixtures of iron oxide with or without Z were added to NPX solution and suspended at least 30 min previous H_2O_2 addition from a fresh daily solution. Similar protocol was carried out for experiments under irradiated conditions. Aqueous slurry was placed in a batch glass vessel and maintained constantly stirred. The solution was

Table 1
Chemical properties of NPX

Characteristic	NPX
Absorption spectrum in deionized water (NPX 10 mg L ⁻¹)	
IUPAC name	(2s)-2-(6-methoxynaphthalen-2-yl) propanoic acid
Molecular weight (g mol ⁻¹)	230.259
Molecular Formula	C ₁₄ H ₁₄ O ₃
CAS reference	015,307-86-5
Fusion point °C	153
Water solubility 25 °C (mg L ⁻¹)	15.9
Water solubility 25 °C as sodic salt (mg L ⁻¹)	>100
Partition coefficient Log <i>P</i>	3.18
Vapor pressure (mm Hg)	1.89 × 10 ⁻⁶
Henry constant	3.39 × 10 ⁻¹⁰
Dissociation constant p <i>K</i> _a	4.5

Reference <http://pubschem.ncbi.nlm.nih.gov/summary.cgi?cid=15,639>, visited May 2013.

Table 2
Chemical properties of hyd Fe₂O₃, Fe₂O₃, Fe₃O₄, and ZSM5

	α-Fe ₂ O ₃ ·H ₂ O	α-Fe ₂ O ₃	Fe ₃ O ₄	Na-ZSM5
Commercial name	Hydrated hematite	Hematite	Magnetite	PZ-2/25
Appearing				
SiO ₂ /Al ₂ O ₃ [mol/mol]	–	–	–	24
Crystal size [μm]	–	–	–	1.5
Pore Ø [nm]	–	–	–	0.55
Purity [%]	85–88	94–97	97–99	na
Particle size [<i>d</i> ₅₀]	na	na	na	<3
Average pore size [Å]	1.39	1.02	1.44	3.21
Surface area [m ² /g]	11.39	8.45	12.36	329.33
Na ₂ O [wt.%]	–	–	–	1.8
Bandgap (eV)	2.4	2.2	2.1	–

Reference: www.zeochem.ch and Suministro de Especialidades SA de CV.

na: not available.

pumped and reflowed toward two cylindrical Pyrex photoreactor (200 mL of irradiated volume) parallel and sequenced placed into the SunTest (Atlas) equipped with a Xenon arc lamp (300–800 nm,

2,700 kJ/hm²). The temperature of the solution was maintained to 25 °C with a thermostatic bath through the glass-jacketed batch vessel. Periodical samples were withdrawn and filtrated with a 0.45 μm HAWP

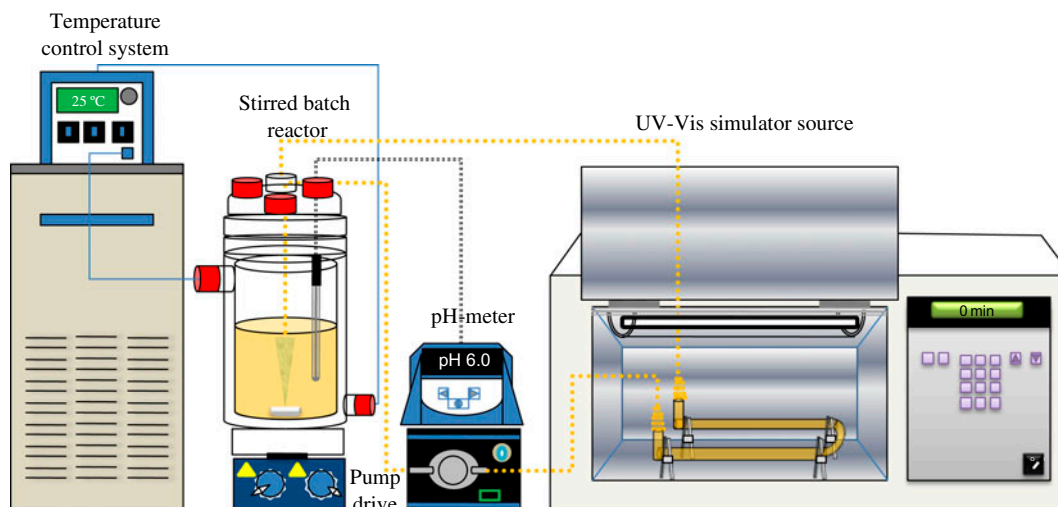


Fig. 1. Equipment and instruments employed.

Millipore filter previous analytical procedures. Fig. 1 depicts the equipment and instruments employed.

3. Results and discussion

In order to evaluate the isolated non-catalytic effects with iron oxides, H_2O_2 , and UV-vis irradiation, exploratory previous experiments were carried out. Moreover, the Fenton-like and photo-Fenton-like reaction were developed by use of initial 10 mg L^{-1} of NPX concentration, $13 \pm 1.3 \text{ mM}$ of H_2O_2 , 0.05 g L^{-1} of iron oxide minerals (hyd Fe_2O_3 , Fe_2O_3 and Fe_3O_4), and 0.1 g L^{-1} of Z unless otherwise specified. The concentrations were selected from former related works by the use of the Fenton reaction [3].

3.1. Exploratory experiments

The lone presence of H_2O_2 promotes degradation of 76% of NPX sodic salt (30 mg L^{-1} initial concentration), especially at a prolonged exposition time (72 h) and high H_2O_2 concentration (147 mM) with a concomitant 20% of DOC reduction. Even high removal of NPX was observed by direct oxidation with H_2O_2 at extended contact time this treatment is not an economically sustainable option due to the H_2O_2 residual composition in the final effluent (more than 80%) as well as its non-biodegradable character. On the other hand, the adsorption phenomena of 10 mg L^{-1} of NPX on 0.1 g L^{-1} of Z was negligible (less than 0.1%) after 24 h of isothermal (25°C) and constant suspended conditions. PZC of Z is around 3.5 and pK_a value of NPX is 4.5. At $\text{pH } 6.5 \pm 0.5$, Z surface and NPX compounds are negatively charged and the electrostatic interaction is not the dominant effect between both reagents. In

addition, NPZ adsorption was not observable due to Z having a crystal size of 1.5 microns has only micropores with the diameter of 0.55 nm, so most of the Z surface is not available for large molecules such as NPX. On the same way, evidence of some NPX complex ligand to iron oxide species (0.05 g L^{-1}) at $\text{pH } 6.5 \pm 0.5$ was not detectable. Initial NPX concentration remained constant after well-stirred contact within 24 h in dark and isothermal conditions for each type of iron oxide employed. The latter was not unexpected due the partial negative charge of both NPX (in ionic form and highly soluble) and iron oxide surfaces ($\text{PZC} > 6$ [26]). Therefore, the promotion of neither electrostatic interaction nor tendency to create organic complexes was observed.

On the other hand, NPX was degraded 70% by photolysis process in 120 min of UV-vis irradiation with an initial degradation rate of $0.4 \mu\text{mol L}^{-1} \text{ min}^{-1}$

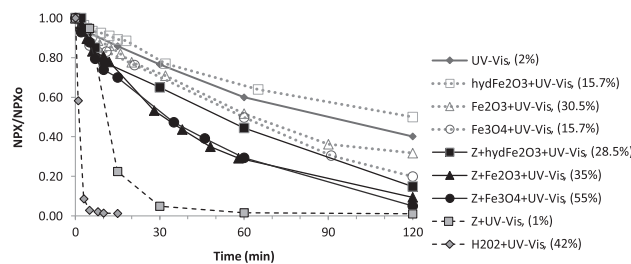


Fig. 2. NPX kinetic depletion and DOC removal (in parenthesis) under UV-vis irradiation in presence of (\square) hyd Fe_2O_3 , (\triangle) Fe_2O_3 , (\circ) Fe_3O_4 , (\blacksquare) Z + hyd Fe_2O_3 , (\blacktriangle) Z + Fe_2O_3 , and (\bullet) Z + Fe_3O_4 , (\blacksquare) Z and (\blacklozenge) H_2O_2 . Operational conditions: initial 10 mg L^{-1} of NPX concentration, $13 \pm 1.3 \text{ mM}$ of H_2O_2 , 0.05 g L^{-1} of iron oxide minerals (hyd Fe_2O_3 , Fe_2O_3 , and Fe_3O_4), and 0.1 g L^{-1} of Z. $\text{pH } 6.5 \pm 0.5$.

and NPX half-life degradation in 90 min (see Fig. 2). NPX shows an absorption band above 340 nm (see Table 1) and its photolysis has been previously examined [27,28]. Photo-transformation of NPX leads an important formation of by-products remained as DOC (decreasing in our experiments less than 2%) in the final effluent. As reported by DellaGreca et al. [27], several photoproducts, such as dimmer compositions, were more toxic than NPX. Therefore, in spite of a significant elimination of initial NPX by the sole UV-vis irradiation, this does not represent a sustainable method to degrade this contaminant from water.

3.2. UV-vis-based processes

The mechanical mixture under dark conditions between Z and each iron oxide or H₂O₂ (13 ± 1.3 mM of H₂O₂) showed a negligible change on the initial concentration of NPX along 120 min of contact. As explained in Section 3.1, the last was consequence of the negligible adsorption or metal complex formation previously observed in presence on Z or iron oxide materials as well as the short oxidation time in presence of H₂O₂.

In contrast, for the UV-vis-based processes in combination with iron oxide species, H₂O₂, and Z showed significant differences in NPX kinetic decay. Fig. 2 shows the NPX kinetic depletion and % of DOC reduction (in parenthesis) after 120 min under UV-vis irradiation in presence of hyd Fe₂O₃, Fe₂O₃, Fe₃O₄, Z + hyd Fe₂O₃, Z + Fe₂O₃, Z + Fe₃O₄, Z, and H₂O₂. The efficiency in degrading NPX increased in the order UV-vis < iron species + UV-vis < Z + iron species + UV-vis < Z + UV-vis < H₂O₂ + UV-vis (with a concomitant initial NPX degradation rate of 0.4 < 0.5 < 1.2 < 3.6 < 9 μmol L⁻¹ min⁻¹). In all cases, final concentration of NPX remains below 50%. The irradiation of Fe₂O₃ and Fe₃O₄ degrades more than 70% of initial NPX with a concomitant mineralization between 30 and 15%. Regarding the iron oxide, the relative order of reactivity toward NPX oxidation was Fe₃O₄ ≥ Fe₂O₃ > hyd Fe₂O₃. The photochemical properties and differences between iron oxides are associated with the photoproducing e⁻/h⁺ activity [23,29] in addition of the contribution of parallel reactions, not only reacting with NPX but also with by-products of NPX photolysis. For instance, Fe₂O₃ (band gap around 2.2 eV) has shown potential semiconductor character for interfacial electron transfer. Similar photochemical properties of Fe(III)-OH complexes, Fe(III) oxides, or Fe(III) hydroxides have been widely shown [29,31], particularly for oxides such α-Fe₂O₃, γ-Fe₂O₃, α-FeOOH, β-FeOOH, and γ-FeOOH. In the case of NPX depletion, even any

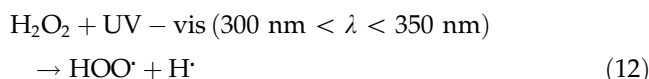
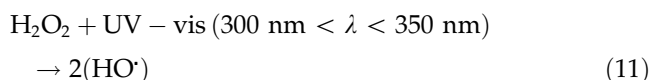
remarkable evidence of initial Fe-NPX ligand was observed, it is possible to assure that initial photoelectronic rearrangement on the illuminated iron surface reach the NPX and/or NPX by-products (also presents from simultaneous photolysis of NPX) in the proximity of the slurry. Special activity through the carboxylic moiety is strongly suggested due to the DOC elimination observed between 15 and 30%.

In analogous experiments in the presence of Z, the notable increase the DOC elimination is observed in particular cases for hematite and magnetite species with 35 and 55% mineralization. The last increase is achieved due to concurrent adsorptive process of by-products with essential hydrophobic character such as polymers with high molecular weight (dimmer compounds) previously reported by Mendez-Arriaga et al. [28]. An unusual increase in the pH (one unit) during the degradation, with iron oxides with and without Z, helps to clarify the carbonate formation as similar as the observed by heterogeneous photocatalysis degradation with TiO₂ under irradiated conditions. The hydrophobic compounds, more than the soluble acid by-products, promote an increase in elimination of DOC by adsorptive stage in presence of Z. It is interesting to emphasize that the activity of hyd-Fe₂O₃ was the lowest observed compared to with those by the use of Fe₂O₃ and Fe₃O₄ with and without Z presence. The lower activity of hyd-Fe₂O₃ has been previously shown by authors in degradation of several pollutants [17]. For example, several reports indicate that Fe(III) oxides—such Fe₂O₃, FeO-OH, and ferrihydrite—are less reactive than their Fe(II) counterparts—such Fe₃O₄, FeO and pyrite[6,9].

In presence of the sole Z, NPX is totally depleted but in a low extent mineralized, less than 1%. The latter is attributed to the contribution of NPX photolysis process accelerated by the photo reflective character of the brilliant white Z powder under UV-vis illumination. Any HO· yield can be suggested due to the high remain DOC was observed after processes. The Z + UV-vis process accelerates the photolysis of NPX by the promotion of absorption of photons reflected from the Z surface through the illuminated area. Unimportant adsorption stage in Z material, from a non-radical attack with formation of soluble stable by-products is the main effect of the Z + UV-vis processes. Thus, the sole photolysis of NPX plays a significant role in its degradation added to parallel reactions in presence of iron oxide species and Z. Moreover, the most relevant remark in this series of experiments was the significant degradation of NPX in the simple presence of H₂O₂ under irradiated conditions. Initial rate of consumption of H₂O₂ was 21 μmol L⁻¹ min⁻¹ and 75% remained after 120 min of irradiation. The photolysis

of H_2O_2 under solar simulated irradiation has been showed previously [32,33]. A significant generation of highly reactive HO^\bullet species is reached from the overlap of the emitted UV–vis spectrum and the ability to be absorbed by H_2O_2 . Under our experimental technical conditions ($>300\text{ nm}$ and Pyrex glass photoreactor) the overlap is placed approximately from 300 up to 350 nm.

Thus, the photochemical cleavage of hydrogen peroxide to yield hydroxyl radicals and/or other radical species by solar light absorption acts as source of radical species [3]:



Thus, the HO^\bullet yield is efficiently used for degradation not only of NPX by direct hydroxylation but also by photo induced by-products. The H_2O_2 photolysis reached significant DOC removal of 42%. This important increase in the DOC removal is attributed to the scavenger character of NPX—similar to other non-steroidal anti-inflammatory compounds [33]—following a remarkable hydroxylation process in aqueous phase with further decarboxilation step. In presence of every material (Z or iron oxide species), an early radical deactivation with an unproductive HO^\bullet attack yield is

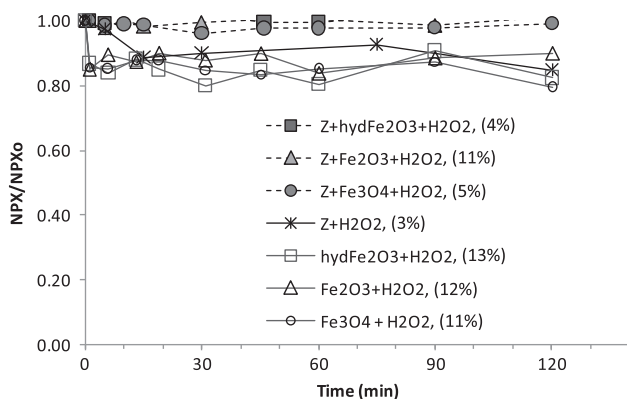


Fig. 3. NPX kinetic depletion and DOC removal (in parenthesis) in Fenton-like reaction: (\square) hyd Fe_2O_3 , (\triangle) Fe_2O_3 , (\circ) Fe_3O_4 , (\blacksquare) Z + hyd Fe_2O_3 , (\blacktriangle) Z + Fe_2O_3 , (\bullet) Z + Fe_3O_4 . Operational conditions: initial 10 mg L^{-1} of NPX concentration, $13 \pm 1.3\text{ mM}$ of H_2O_2 , 0.05 g L^{-1} of iron oxide minerals (hyd Fe_2O_3 , Fe_2O_3 and Fe_3O_4) and 0.1 g L^{-1} of Z. $\text{pH } 6.5 \pm 0.5$.

observed by the main photo competition among H_2O_2 , Z, iron species, and NPX by itself.

3.3. Fenton-like reaction

Experiments of Fenton-like reaction by the use of commercial iron oxide species were carried out. Fig. 3 shows the NPX kinetic depletion and % of DOC reduction (in parenthesis) after 120 min for Fenton-like aqueous reaction (hyd Fe_2O_3 , Fe_2O_3 , Fe_3O_4 , and H_2O_2 with and without Z). A Fenton-like aqueous reaction results in an insignificant degradation of NPX in presence or absence of Z. In the case of iron oxide species, an early initial almost constant reduction of NPX (within first minutes) of 17% with a concomitant approximately 11–13% DOC removal is observed. An erratic NPX concentration behavior is followed during the experiment by possible complex-adsorption-desorption process without further oxidative reaction with H_2O_2 and a sole formation of aqueous complex on the iron oxide surfaces. A low initial reduction of H_2O_2 was detected along the experiment (0.014 , 0.009 , and $0.010\text{ mmol L}^{-1}\text{ min}^{-1}$ for hyd Fe_2O_3 , Fe_2O_3 , and Fe_3O_4 respectively) but no degradation can be addressed along 120 min. The only disappearance of H_2O_2 is not a valid reaction test to insure the occurrence of Fenton chemistry due to the most active catalyst for H_2O_2 decomposition is not the one that generates hydroxyl radicals. It depends on the array of pathways available for H_2O_2 decomposition [17]. Consumption of H_2O_2 is due to hydrolysis and formation of hydroperoxide complexed to metal without remarkable radical formation. Moreover, at using pH any possible iron leaching into the bulk phase can be suggested, thus the slight consumption of H_2O_2 cannot be addressed to some Fenton-like reaction. Other authors also suggest that, even in observations with 7% of iron leached, the Fe concentration was not major responsible of catalytic activity response observed [34]. In correspondence with several authors [16–18], any noteworthy Fenton-like reaction was observed in presence of iron oxides for degradation of NPX due to ineffective H_2O_2 consumption without concomitant HO^\bullet generation.

In presence of Z, the initial adsorption/complex formation with NPX is reduced (only 6–8%) with a concomitant DOC reduction of 3%. The presence of Z avoids interactions between NPX, iron oxide species, and H_2O_2 . Furthermore, the H_2O_2 consumption is reduced only for Fe_3O_4 ($0.008\text{ mmol L}^{-1}\text{ min}^{-1}$), also without further evidence of HO^\bullet formation. Our observations are also close to evidences reported by Costa et al. [16] and Lim et al. [7] among others. They observed that the presence of commercial Fe_3O_4 and

Fe^0 (3 mg mL^{-1}) and their mechanical mixtures are nearly inactive for the decomposition of H_2O_2 (0.3 mol L^{-1}) in the degradation of dye model compounds (10 mg L^{-1}) at $\text{pH } 6 \pm 0.2$. Also, Lim et al. [7] probed that commercial Fe_2O_3 and Fe_3O_4 powders did not show any significant activity for the degradation of reactive black 5 (100 mg L^{-1}) based on the H_2O_2 (5 mmol L^{-1}) negligible consumption. Kwan et al. [6] evidenced the rapid loss of HO_2/O_2^- with a concomitant absence of HO^\bullet on the oxide surface-initiated solution chain reaction in a non-radical initiated mechanism. As Andrezzi et al. [8] propose, the mechanism would involve more abundant surface species, such sorbed hydrogen peroxide or substrate arrays, than the active catalytic Fe(II) surface sites. Thus, while reaction of the bulk solution radicals with iron oxide surfaces cannot be important due to the collision frequency limitations, such reactions are plausible for radicals formed in the surface film. Last examples have denoted the inefficacy of Fenton-like reaction by use of iron oxides, however in contrast other authors assure that $\text{FeO}\cdot\text{Fe}_2\text{O}_3$ (magnetite, 25 mg mL^{-1}) catalyzes the decomposition of H_2O_2 (100 mM) with HO^\bullet formation sufficiently to reach high catalytic activity for decolorization (38–99%) of eight dyes at $\text{pH } 6.6$ [10]. In such case, metal ions forms firstly a complex with H_2O_2 on the surface of the catalyst. Then, the catalytic activity of oxides observed by Baldrian et al. [10] is not closely and directly connected with the formation of reactive hydroxyl radicals but also by the previous production of other reactive species (e.g. H_2O_2 metal complexes) playing an significant role as chelators on the oxides contrasted with the initial minor adsorption fraction. Similar appreciations have been showed by other authors for the particular case of the goethite mineral [6,8]. However, a general model that predicts these rates under a broad range of conditions has not been developed.

Therefore, yield of HO^\bullet in systems based on the catalytic decomposition of H_2O_2 by iron oxide species and their mechanistically radical approach are still controversial in the open available literature and come into sight to be strong dependent of the substrate (chelating or adsorption on iron species if any), H_2O_2 amount, nature and type of iron oxide and pH , among others. The experience probed in this investigation evidences that attribution of HO^\bullet radical yield is not possible to confirm based in the presence of $\text{hyd-Fe}_2\text{O}_3$, Fe_2O_3 , and Fe_3O_4 as catalyst for decomposition of H_2O_2 at *circum* neutral pH . However, the reduction of NPX (less than 10%) can be related to formation of initial organic complex involving the presence of H_2O_2 on the iron oxide.

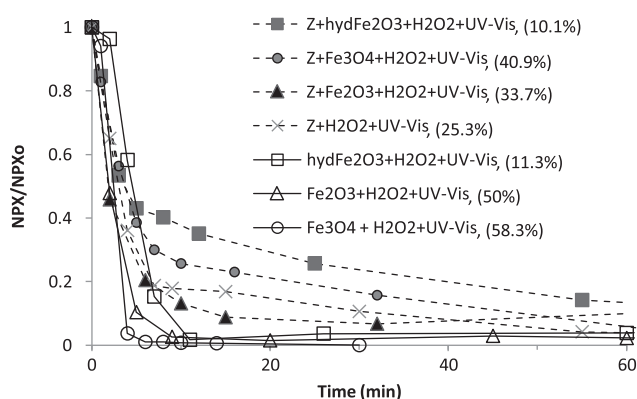


Fig. 4. NPX kinetic depletion and DOC removal (in parenthesis) in photo-Fenton-like reaction in presence of (\square) $\text{hyd Fe}_2\text{O}_3$, (\triangle) Fe_2O_3 , (\circ) Fe_3O_4 , (\blacksquare) $\text{Z} + \text{hyd Fe}_2\text{O}_3$, (\blacktriangle) $\text{Z} + \text{Fe}_2\text{O}_3$, (\bullet) $\text{Z} + \text{Fe}_3\text{O}_4$, and (\blacksquare) blank Z without iron specie. Operational conditions: initial 10 mg L^{-1} of NPX concentration, $13 \pm 1.3 \text{ mM}$ of H_2O_2 , 0.05 g L^{-1} of iron oxide minerals ($\text{hyd Fe}_2\text{O}_3$, Fe_2O_3 and Fe_3O_4), and 0.1 g L^{-1} of Z . $\text{pH } 6.5 \pm 0.5$.

3.4. Photo-Fenton-like reaction

Fig. 4 shows the NPX kinetic depletion and % of DOC reduction (in parenthesis) after 120 min for photo-Fenton-like aqueous reaction ($\text{hyd Fe}_2\text{O}_3$, Fe_2O_3 , Fe_3O_4 , and H_2O_2 with and without Z). In all the cases, total depletion of NPX was reached within ≈ 60 min. However, remarkable differences were observed according the DOC removal. Under irradiated conditions, iron oxide species and H_2O_2 promote the highest initial degradation rates remarkably enhanced in the case of the use of hematite: 13, 18, and $14 \mu\text{mol L}^{-1} \text{ min}^{-1}$ for $\text{hyd Fe}_2\text{O}_3$, Fe_2O_3 , and Fe_3O_4 , respectively. In all cases, with presence of Z the initial degradation rates are reduced 32, 22, and 42% for $\text{hyd-Fe}_2\text{O}_3$, Fe_2O_3 , and Fe_3O_4 correspondingly. An increase of ≈ 10 , 20, and 42% of DOC removal was observed when Z was not present in the mechanical mixture for $\text{hyd-Fe}_2\text{O}_3$, Fe_2O_3 , and Fe_3O_4 , respectively. H_2O_2 consumption increases in the case of Fe_2O_3 and Fe_3O_4 in absence of Z (0.089 and $0.047 \text{ mmol L}^{-1} \text{ min}^{-1}$, respectively).

In contrast, under dark conditions, the presence of Z inactivates the H_2O_2 reactivity. The decomposition of H_2O_2 in the case of $\text{hyd-Fe}_2\text{O}_3$ showed a negligible difference between dark and illuminated conditions (0.014 and $0.015 \text{ mmol L}^{-1} \text{ min}^{-1}$, respectively). The relative order of reactivity toward NPX oxidation was $\text{hyd Fe}_2\text{O}_3 < \text{Fe}_2\text{O}_3 \leq \text{Fe}_3\text{O}_4$. Reactivity of photo-Fenton-like process is mainly attributed to the initial photoactive aqua organic complex formation involving NPX, iron surfaces, and H_2O_2 . As shown in point 3.2, the photochemical properties of iron oxides are associated

to the analogous activity of photoproducing e^-/h^+ couple observed in the photocatalytic semiconductors as TiO_2 . The electron transfer step is rate-limiting, and the rate constant for this step depends on the surface properties of the metal oxide and the nature of the complexation ligands. Even more, the combination of simultaneous photoactive processes (such as NPX or H_2O_2 photolysis) promotes a synergistic effect on NPX degradation. H_2O_2 is an electron acceptor and reacts with the electrons of the photo-activated surface of the catalyst or photo-by-products:



The initial favored condition of a complex aqua complex organic array between NPX, iron surface, and H_2O_2 support in a strong manner the photo-electron interchange involving a main formation of HO^\bullet radical along the reaction previous non-radical initial mechanism. Presence of Z hinders the degradation of NPX due to photogenerated electrons are deactivated also on Z surface without further reaction. In presence of Z, the DOC removal decreases, especially in the case of Fe_2O_3 and Fe_3O_4 (reduction of 18 and 42% respectively). The oxidative stress of NPX and the by-products with hydrophilic character and without further absorbable disposition on Z also decelerates the mineralization by radical attack. The sole presence of Z reaches a DOC removal of 25% with an initial H_2O_2 consumption of $0.024 \text{ mmol L}^{-1} \text{ min}^{-1}$ and initial NPX degradation rate of $7 \text{ mmol L}^{-1} \text{ min}^{-1}$. On this case, the degradation of NPX corresponds to a simultaneous effect of photolytic process of NPX and oxidative promotion from HO^\bullet generation by H_2O_2 photolysis.

3.5. Biodegradability measurements

BOD_5 measures were carried out for all experiments tested previous total depletion of H_2O_2 . A non-biodegradable character was observed for initial 10 mg L^{-1} NPX dissolution with a BOD_5 of 0.5 mg L^{-1} . The low BOD_5 of initial NPX obeys to the recalcitrant character of NPX to biological degradation. Increase of the biodegradability character of treated solution was observed only in experiments: (1) irradiated iron oxides (hyd Fe_2O_3 , Fe_2O_3 , and Fe_3O_4), (2) H_2O_2 photolysis, (3) $Z + H_2O_2 + UV\text{-vis}$, and (4) $Z + H_2O_2$ at 4, 14, 16, and 21-folds higher than the observed for initial substrate (2, 7, 8, and 10.5 mg L^{-1} , respectively). The increase in the biodegradability in such process was not related to the final DOC observed. Similar or lower BOD_5 values compared to the initial BOD_5 were

observed in cases with high DOC removal (i.e. photo-Fenton-like with hematite and magnetite in absence of Z). Due to the well-differentiated phenomena and/or transformation mechanism in each subsystems studied, the by-products and pathways affected in a strong manner the final effluent character and biodegradable properties. After total depletion of NPX the final composition of effluent with hydrophilic and hydrophobic by-products determines the biodegradable character. A deep study including the identification of by-products per processes as well as the complementary toxicity analysis of final effluent is actually carried out as complement of this study. Furthermore, the Fe-ZSM5 synthesized material as well as its reusability under variable irradiated area is the focus of our current investigation.

4. Conclusions

Control experiments showed that neither hyd- Fe_2O_3 , nor Fe_2O_3 , nor Fe_3O_4 nor Z has any complex or absorbable ability on NPX at $pH 6.5 \pm 0.5$. H_2O_2 direct oxidation is effective to degrade more than 50% of initial NPX only at concentrations higher than 147 mM in extended periods (longer than 72 h) without final biodegradable character of the effluent. Photolysis process degrades more almost 50% of the initial NPX without further mineralization. Under presence of Z, photolysis of NPX is accelerated, however DOC removal is maintained at low extent (1%). The UV-vis + H_2O_2 process reaches a DOC removal (42%) due to the main HO^\bullet scavenger character of NPX and the further oxidative stress of the by-products with an improved final BOD_5 observed of 7 mg L^{-1} . The Fenton-like reaction, in presence or absence of Z and for hydrated hematite, hematite, and magnetite, does not reach any evidence or presence of radicalary mechanism addressed to the aquo-complex formation in presence of H_2O_2 and iron oxide species. Any catalytic behavior of iron oxide species to decompose H_2O_2 in presence of hyd- Fe_2O_3 , either Fe_2O_3 or Fe_3O_4 can be assured. Only in the case of H_2O_2 photolysis, there is an evidenced HO^\bullet formation and attack on NPX, otherwise the H_2O_2 amount remains almost constant without further consumption in the presence of iron oxide species and Z in dark conditions. In contrast, photo-Fenton-like reaction promotes total elimination of initial 10 mg L^{-1} of NPX with a concomitant 50–59% of mineralization in the case of use of Fe_2O_3 and Fe_3O_4 , respectively. Improvement of DOC reduction by adsorption due to the presence of Z was not observed under illuminated conditions, and biodegradable character of final effluent was not improved.

The presence of Z promotes detrimental results in both Fenton-like and photo-Fenton-like cases. Photo-Fenton-like reaction, by use of $\text{hyd-Fe}_2\text{O}_3$, Fe_3O_4 , and Fe_2O_3 is a promise alternative to promote mineralization of NPX reaching total elimination under pH neutral conditions. Residual by-products are not suitable for a post-biological operation due to the probable formation of recalcitrant polymers (likely strong stable dimmers) not further degraded. In contrast, only in the case of use of Z in dark of illuminated circumstances in presence of H_2O_2 increased the biodegradable character of the treated effluent (8 and 10.5 mg L^{-1} , respectively).

Acknowledgment

Authors would acknowledge the support from CICT-Universidad Nacional Autónoma de México (UNAM) and ICYT-DF (Women Fellowship program and project PICSO-11/13) for the doctoral and post-doctoral fellowship. F M-A appreciate the invaluable collaboration of Prof. Albert Ortiz, Dr Fabricio Espejel, Biol. Nora Salinas, Eng. Ernesto Olvera, Eng. Pedro Muñoz, Eng. Roberto Briones, Dr Alfonso Durán, and Dr Simón González to perform this investigation.

References

- [1] D. Fatta-Kassino, S. Meric, A. Nikolaou, Pharmaceutical residues in environmental waters and wastewater: Current state of knowledge and future research, *Anal. Bioanal. Chem.* 399 (1) (2011) 251.
- [2] A. Synder, M. Adam, F. Redding, J. DeCarollis, J. Oppenheimer, E. Wert, Y. Yoon, Role of the membranes and activated carbon in the removal of endocrine disruptors and pharmaceuticals, *Desalination* 202 (2007) 156–181.
- [3] F. Mendez-Arriaga, 2009a. Advanced oxidation process (photocatalysis, photo-Fenton and sonolysis) for removal of pharmaceutical pollutants in water. Doctoral Thesis, Barcelona University, 2009.
- [4] A. Giraldo, G. Penuela, R. Torres-Palma, N. Pino, R. Palominos, H. Mansilla, Degradation of the antibiotic oxolinic acid by photocatalysis with TiO_2 in suspension, *Water Res.* 44(18) (2010) 5158–5167.
- [5] O. González, C. Sans, S. Esplugas, Sulfamethoxazole abatement by photo-Fenton. Toxicity, inhibition and biodegradability assessment of intermediates, *J. Hazard. Mater.* 146 (2007) 459–464.
- [6] W. Kwan, B. Voelker, Influence of electrostatics on the oxidation rates of organic compounds in heterogeneous Fenton systems, *Environ. Sci. Technol.* 38(12) (2004) 3425–3431.
- [7] S. Lin, M. Gurol, Catalytic decomposition of hydrogen peroxide on iron oxide: Kinetics, mechanism and implications, *Environ. Sci. Technol.* 32 (1998) 1417–1423.
- [8] R. Andreozzi, V. Caprio, R. Marotta, Oxidation of aromatic substrates in water/goethite slurry by means of hydrogen peroxide, *Water Res.* 36(19) (2002) 4691–4698.
- [9] E. Garrido-Ramirez, B. Theng, M. Mora, Clays and oxide minerals as catalyst and nanocatalyst in Fenton-like reactions—a review, *Appl. Clay Sci.* 47 (2010) 182–192.
- [10] P. Baldrian, V. Merhautova, J. Gabriel, F. Nerud, P. Stopka, M. Hruby, M. Benes, Decolorization of synthetic dyes by hydrogen peroxide with heterogeneous catalyst by mixed iron oxides, *Appl. Catal. B: Environ.* 66 (2006) 258–264.
- [11] M. Lu, J. Chen, H. Huang, Role of goethite dissolution in the oxidation of 2-chlorophenol with hydrogen peroxide, *Chemosphere* 46 (2002) 131–136.
- [12] H. Huang, M. Lu, J. Chen, Catalytic decomposition of hydrogen peroxide and 2-chlorophenol with iron oxides, *Water Res.* 35 (2001) 2291–2299.
- [13] R. Matta, K. Hanna, S. Chiron, Fenton-like oxidation of 2,4,6-trinitrotoluene using different iron minerals, *Sci. Total Environ.* 385 (2007) 242–251.
- [14] S. Chou, C. Huang, Application of a supported iron oxyhydroxide catalyst in oxidation of benzoic acid by hydrogen peroxide, *Chemosphere* 38 (1999) 2719–2731.
- [15] S. Kong, R. Watts, J. Choi, Treatment of petroleum-contaminated soils using iron mineral catalyzed hydrogen peroxide, *Chemosphere* 37 (1998) 1473–1482.
- [16] R. Costa, F. Moura, J. Ardisson, J. Fabris, R. Lago, Highly active heterogeneous Fenton-like system based on $\text{Fe}^0/\text{Fe}_3\text{O}_4$ composites prepared by controlled reduction of iron oxides, *Appl. Catal. B: Environ.* 83 (2008) 131–139.
- [17] S. Navalon, M. Alvaro, H. García, Review: Heterogeneous Fenton catalysis, silicas and zeolites, *Appl. Catal. B: Environ.* 99 (2010) 1–26.
- [18] L. Guo, F. Chen, X. Fan, W. Cai, J. Zhang, S-doped $\alpha\text{-Fe}_2\text{O}_3$ as a highly active heterogeneous Fenton-like catalyst towards the degradation of acid orange 7 and phenol, *Appl. Catal. B: Environ.* 96 (2010) 162–168.
- [19] J. Melero, F. Martínez, J. Botas, R. Molina, M. Pariente, Heterogeneous catalytic wet peroxide oxidation systems for the treatment of an industrial pharmaceutical wastewater, *Water Res.* 43 (2009) 4010–4018.
- [20] J.J. Pignatello, E. Oliveros, A. MacKay, Advanced oxidation processes for organic contaminant destruction based on the Fenton reaction and related chemistry, *Crit. Rev. Environ. Sci. Technol.* 36 (2006) 1–84.
- [21] I. Arslan-Alaton, F. Gurses, Photo-Fenton-like and photo-fenton-like oxidation of Procaine Penicillin G formulation effluent, *J. Photochem. Photobiol. A: Chem.* 165 (2004) 165–175.
- [22] C. Pulgarin, P. Peringer, P. Albers, J. Kiwi, Effect of the Fe-ZSM-5 zeolite on the photochemical and biochemical degradation of 4-nitrophenol, *J. Mol. Catal. A: Chem.* 95 (1995) 61–74.
- [23] C. Pulgarin, J. Kiwi, Iron oxide mediated degradation, photo-degradation and biodegradation of aminophenols, *Langmuir* 11 (1995) 519–526.
- [24] K. Farjerwerger, T. Castan, J. Foussard, A. Perrard, H. Debellefontaine, Dependence of some operating parameters during the wet oxidation of phenol by hydrogen peroxide with Fe-ZSM-5 zeolite, *Environ. Technol.* 21 (2000) 337–344.
- [25] R. Torres-Palma, F. Abdelmalek, E. Combet, C. Petrier, C. Pulgarin, A comparative study of ultrasonic cavitation and Fenton's reagent for bisphenol A degradation in deionised and natural waters, *J. Hazard. Mater.* 146 (2007) 546–551.
- [26] K. Hanna, T. Kone, G. Medjahdi, Synthesis of the mixed oxides of iron and quartz and their catalytic activities for the Fenton-like oxidation, *Catal. Commun.* 9 (2008) 955–959.
- [27] M. DellaGreca, M. Brignate, M. Isidori, A. Nardelli, L. Previtera, M. Rubino, F. Temussi, *Environ. Chem. Lett.* 1 (2004) 237–241.
- [28] F. Mendez-Arriaga, J. Giménez, S. Esplugas, Photolysis and TiO_2 photocatalytic treatment of naproxen: Degradation, mineralization, intermediates and toxicity, *J. Adv. Oxid. Technol.* 11 (2009) 436–445.
- [29] W. Feng, D. Nansheng, Photochemistry of hydrolytic iron (III) species and photoinduced degradation of organic compounds. A mini review, *Chemosphere* 41 (2000) 1137–1147.
- [30] B. Faust, M. Hoffmann, Photoinduced reductive dissolution of $\alpha\text{-Fe}_2\text{O}_3$ by bisulphite, *Environ. Sci. Technol.* 20 (1986) 943–948.

- [31] K. Cunningham, M. Golderberg, E. Weiner, Mechanism for aqueous photolysis of adsorbed benzoate and succinate on iron oxyhydroxide (goethite) surfaces, *Environ. Sci. Technol.* 22 (1988) 1090–1097.
- [32] D. Kritikos, N. Xekoekoelotakis, E. Psillakis, D. Mantzavinos, Photocatalytic degradation of reactive black 5 in aqueous solutions: effect of operating conditions and coupling with ultrasound irradiation, *Water Res.* 41(10) (2007) 2236–2246.
- [33] F. Mendez-Arriaga, I. Maldonado, J. Gimenez, S. Esplugas, S. Malato, Abatement of ibuprofen by solar photocatalysis process: Enhancement and scale up, *Catal. Today* 144 (2009) 112–116.
- [34] G. Centi, S. Perathoner, T. Torre, M. Verduna, Catalytic wet oxidation with H_2O_2 of carboxylic acids on homogeneous and heterogeneous Fenton-type catalysis, *Catal. Today* 55 (2000) 61–69.